Sol-gel synthesis of $LaFeO_3$ nanoparticles for gas sensing application

Monali E. Niphade[1], Uglal P. Shinde[2], Arun V. Patil[3]

[1-3] Research Centre in Electronic Science, Mahatma Gandhi Vidyamandir's Loknete Vyankatrao Hiray Arts, Science and Commerce College, Panchavati, Nashik-03, Affiliated to Savitribai Phule Pune University, Pune, Maharashtra - 422003, India.
[2]M.J.M. Arts, Commerce and Science College, Karanjali, Tal. Peth, Dist. Nashik, Affiliated to SPPU, Pune, Maharashtra - 422208, India.
[3]Department of Physics, MGV's, Arts, Science and Commerce College, Manmad, Nashik, Affiliated to Savitribai Phule Pune University, Maharashtra, India

Abstract:
In the present research work the $LaFeO_3$ nanoparticles were successfully synthesis by sol-gel method. $LaFeO_3$ nanoparticles were successfully synthesized via a sol-gel route using ferric nitrate nonahydrate and lanthanum nitrate hexahydrate as precursors, with ascorbic acid dissolved in ethylene glycol and deionized water as the chelating agent. The obtained gel was dried, and calcined at 400 °C to achieve phase-pure $LaFeO_3$ nanoparticles. These nanoparticles were used for the fabrication of thick films by the conventional screen-printing method on glass substrates, employing a 70:30 ratio of inorganic to organic binders (ethyl cellulose and butyl carbitol acetate) to form a thixotropic paste. The prepared films were annealed at 400 °C to enhance stability and remove organic residues. The structural, morphological, and compositional properties of the films were systematically analyzed using X-ray Diffraction (XRD), Field Emission Scanning Electron Microscopy (FESEM) and Energy Dispersive X-ray Spectroscopy (EDX). Gas sensing performance was investigated against selected gases, including NH_3, LPG, CO, ethanol, and SO_2. The $LaFeO_3$ films exhibited maximum sensitivity (58.13%) and excellent selectivity toward ethanol gas at 160 °C with 1000 ppm concentration, along with response and recovery times of 23 and 104 seconds, respectively. The result demonstrate the potential of $LaFeO_3$ thick films as efficient ethanol gas sensors with good stability and reproducibility.

Keywords: $LaFeO_3$ nanoparticles, sol-gel method, thick films, screen printing, structural characterization, gas sensing, ethanol detection, perovskite oxides.

1. Introduction

The continuous increase in environmental pollution, industrialization, and rapid urbanization has raised significant concerns over the emission of hazardous gases into the atmosphere, which adversely affect both human health and ecological balance [1, 2]. Toxic and flammable gases such as ammonia (NH_3), carbon monoxide (CO), sulfur dioxide (SO_2), liquefied petroleum gas (LPG), and volatile organic compounds like ethanol (C_2H_5OH) are released during industrial processes, vehicular emissions, domestic cooking, and various chemical reactions [1-3]. Exposure to these gases, even at low concentrations, can cause severe respiratory and cardiovascular problems, while prolonged inhalation may lead to chronic diseases or fatal outcomes. Therefore, the demand for highly sensitive, selective, and reliable gas sensors has grown tremendously to ensure environmental monitoring, workplace safety, and pollution control [4, 5]. Among the various materials explored for gas sensing, semiconducting oxides have attracted significant research interest due to their tunable structural, electronic, and catalytic properties [5, 6]. In particular, perovskite oxides with the general formula ABO_3 have emerged as promising candidates owing to their versatile crystal structure, chemical stability, and ability to host multiple cation substitutions that improve sensing performance [7, 8].

Lanthanum ferrite ($LaFeO_3$), an orthorhombic perovskite-type oxide, has gained attention as an efficient sensing material due to its unique structural and electronic properties [9, 10]. Being a p-type semiconductor,

$LaFeO_3$ possesses a narrow band gap (~2.1 eV), high thermal stability, and excellent catalytic activity, making it suitable for detecting reducing gases at relatively low operating temperatures. The perovskite structure of $LaFeO_3$ provides a flexible lattice framework where the A-site (La^{3+}) and B-site (Fe^{3+}) ions can be easily tuned or substituted with other elements, thereby enhancing surface reactivity and charge carrier mobility. Furthermore, the presence of oxygen vacancies in $LaFeO_3$ plays a vital role in gas sensing, as they act as active sites for gas adsorption and redox reactions [10, 11]. The combination of high oxygen mobility, catalytic behavior, and p-type conduction mechanism enables $LaFeO_3$ to respond efficiently to a wide range of gases. It is considered an environmentally friendly material compared to toxic or expensive transition metal oxides, which adds to its potential for large-scale sensing applications. To fully exploit the gas sensing potential of $LaFeO_3$, the synthesis of nanoparticles with controlled morphology, crystallinity, and surface properties is crucial. Several methods have been reported for the preparation of $LaFeO_3$ nanoparticles, including solid-state reaction, hydrothermal synthesis, sol-gel, co-precipitation, combustion, and spray pyrolysis techniques. Among these, the sol-gel method stands out as an efficient, low-cost, and versatile approach to obtain nanosized powders with high purity and homogeneity [11, 12]. The sol-gel process involves the transition of a colloidal suspension (sol) into a solid (gel) through hydrolysis and polycondensation reactions of metal precursors. By carefully controlling the chelating agents, and calcination parameters, the sol-gel method enables the synthesis of highly crystalline nanoparticles with tailored surface area and porosity, which are essential for enhancing gas adsorption and catalytic activity [12, 13].

Gas sensing performance is highly dependent on the interaction between target gases and the surface of the sensing material. In the case of p-type $LaFeO_3$, the sensing mechanism is governed by the adsorption of oxygen species on the film surface, which captures electrons from the conduction band and increases hole concentration, thereby modulating the resistance of the material [14, 15]. When exposed to reducing gases such as ethanol, the adsorbed oxygen species react with the gas molecules, releasing electrons back into the material and decreasing hole concentration, which leads to a measurable change in electrical resistance. The sensitivity, selectivity, response time, recovery time, and stability of the sensor are critical parameters that determine its practical applicability [15, 16].

In the present study, ascorbic acid was employed as a chelating agent along with ethylene glycol (EG) and deionized water to stabilize the precursor solution and facilitate the formation of a homogeneous gel through the sol–gel route. The subsequent calcination process effectively removed organic residues and led to the development of orthorhombic $LaFeO_3$ nanoparticles with well-defined crystalline characteristics. These nanoparticles were further utilized to fabricate thick films, which were systematically investigated for their gas sensing performance.

2. Materials and methods

2.1 Sol–gel synthesis of $LaFeO_3$ nanoparticles

$LaFeO_3$ nanoparticles were synthesized via a sol–gel route. Initially, 4.4 g of ascorbic acid was dissolved in a mixed solvent of ethylene glycol (EG) and deionized water in a 1:4 molar ratio at room temperature, serving as a chelating and stabilizing medium. Stoichiometric amounts of ferric nitrate nonahydrate [$Fe(NO_3)_3 \cdot 9H_2O$] and lanthanum nitrate hexahydrate [$La(NO_3)_3 \cdot 6H_2O$] were added gradually under continuous stirring to ensure complete dissolution [18]. The resulting homogeneous solution was heated to 80 °C under constant agitation until the formation of a dark brown gel. The gel was desiccated for 9 h to remove excess moisture, followed by grinding to obtain fine precursor powder [10, 17]. The powder was calcined in a muffle furnace at 400 °C for 3 h to yield crystalline $LaFeO_3$ nanoparticles.

2.2 Preparation of $LaFeO_3$ thick films

The synthesized $LaFeO_3$ nanoparticles were used for the fabrication of thick films using the conventional screen printing technique. Glass substrates were chosen as deposition bases and cleaned sequentially with acetone and double-distilled water to remove impurities and ensure good adhesion. A thixotropic paste was prepared by mixing $LaFeO_3$ nanoparticles with organic binders in a 70:30 ratio of inorganic to organic content. Ethyl cellulose (EC) and butyl carbitol acetate (BCA) were employed as temporary binders to impart the desired rheological properties for screen printing. The prepared paste was deposited on the glass substrates to

form uniform films. After printing, the films were dried under an infrared (IR) lamp for 20–30 min to remove volatile impurities and ensure compactness [19, 20]. Finally, the dried films were annealed at 400 °C for 2 h in a muffle furnace to remove organic binders and enhance film adhesion, crystallinity, and stability.

2.3 Characterization techniques

The structural, morphological, and compositional characterizations of the synthesized $LaFeO_3$ nanoparticles and fabricated thick films were carried out using advanced analytical techniques available at the Central Instrumentation Facility (CIF), Savitribai Phule Pune University (SPPU), Pune, Maharashtra. The crystalline structure and phase purity were examined by X-ray diffraction (XRD) using a Bruker D8 VENTURE diffractometer. The surface morphology and particle distribution were studied using Field Emission Scanning Electron Microscopy (FESEM, FEI Nova NanoSEM 450). Elemental composition and chemical purity were analyzed by Energy Dispersive X-ray Spectroscopy (EDS) coupled with the FESEM, equipped with a Bruker XFlash 6I30 detector, ensuring the detection of lanthanum, iron, and oxygen elements in the correct stoichiometry. Functional groups and vibrational modes were identified using Fourier Transform Infrared Spectroscopy (FTIR, PerkinElmer Spectrum model), which revealed characteristic of stretching vibrations along with the absence of organic residues. These characterizations collectively confirmed the successful synthesis of $LaFeO_3$ nanoparticles and their suitability for gas sensing applications.

3. Result and Discussion

Fig. 1 shows the Field Emission Scanning Electron Microscopy (FESEM) micrographs of $LaFeO_3$ nanoparticles recorded at different magnifications, highlighting their surface morphology, particle distribution, and microstructural features.

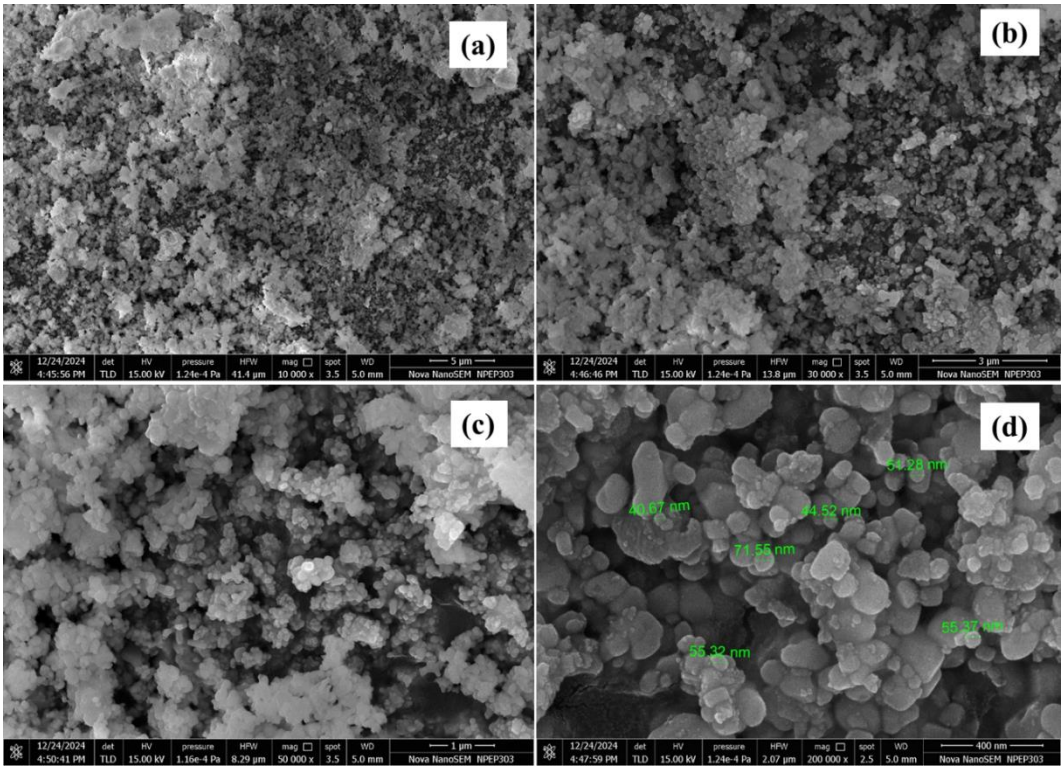

Fig. 1. FESEM micrographs of $LaFeO_3$ nanoparticles at (a) 10k, (b) 30k, (c) 50k & (d) 200k magnifications

At lower magnification 10k (Fig. 1a), the nanoparticles appear to form an interconnected network with noticeable porosity, indicating agglomeration of finer crystallites into larger clusters. Increasing the magnification to 30k (Fig. 1b) provides a clearer view of the granular morphology, where nanoparticles are closely packed but still maintain interparticle voids that contribute to the overall porosity of the material [20, 21]. The 50k magnification image (Fig. 1c) reveals nearly spherical to irregularly shaped nanoparticles with improved clarity, suggesting uniform nucleation and growth during the sol–gel synthesis. At the highest magnification (200k, Fig. 1d), the individual nanoparticles can be distinctly observed, with particle sizes measured in the range of 40–72 nm. The average grain size calculated from these micrographs falls around

~55 nm, which corroborates well with the nanoscale crystallite size derived from XRD analysis. The porous microstructure is particularly advantageous for gas sensing applications, as it facilitates easy diffusion of analyte gases into the sensing layer and enhances the interaction between gas molecules and surface-active sites. The specific surface area of $LaFeO_3$ nanoparticles was determined by BET method (Eq.1) and found to be 2.06 m^2/g [19].

$$S_w = 6/\rho d \qquad \text{(Eq. 1)}$$

Where,

S_w denotes the specific surface area, d represents the diameter of the spherical particles, and

ρ signifies the density of material.

This moderate surface area, coupled with nanoscale particle size and open porosity, significantly improves surface reactivity, thereby contributing to enhanced gas adsorption and catalytic activity. Thus, the FESEM analysis confirms that the synthesized $LaFeO_3$ nanoparticles possess suitable structural and morphological characteristics for efficient gas sensing performance.

Fig. 2 presents the Energy Dispersive X-ray Spectroscopy (EDX) analysis of $LaFeO_3$ nanoparticles, providing elemental composition and spatial distribution of the constituent elements. The EDX spectrum (Fig. 2a) clearly shows distinct peaks corresponding to lanthanum (La), iron (Fe), and oxygen (O), which are the expected elements in $LaFeO_3$. The quantitative analysis reveals that La contributes 65.49 wt. % (31.70 at.%), Fe contributes 25.59 wt.% (30.81 at.%), and O contributes 8.92 wt.% (37.49 at.%). These values confirm the successful incorporation of the desired elements in near-stoichiometric proportion, thereby validating the purity of the synthesized nanoparticles [18, 19]. No additional impurity peaks were observed in the spectrum, which indicates that the synthesis process yielded high-purity $LaFeO_3$ without contamination from other phases or residual precursors.

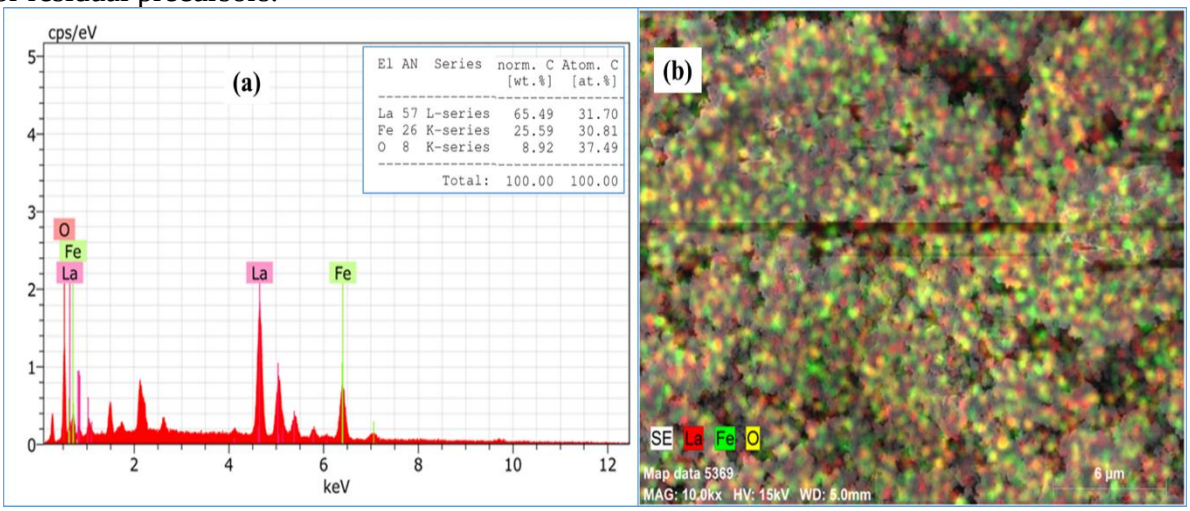

Fig. 2. (a) EDX spectra, & (b) mapping image of $LaFeO_3$ nanoparticles

The elemental mapping image (Fig. 2b) further supports the uniform distribution of La, Fe, and O throughout the nanoparticle matrix. The red, green, and yellow colorations represent La, Fe, and O, respectively, and their homogeneous dispersion across the scanned area demonstrates that the elements are well-integrated within the lattice structure of the nanoparticles. Such a uniform distribution is critical for ensuring consistent physical and chemical properties, which in turn improves the reliability of the material for functional applications such as gas sensing. The absence of localized clusters or segregation of elements indicates effective mixing during the sol–gel synthesis process, followed by proper thermal treatment that stabilized the orthorhombic perovskite phase of $LaFeO_3$ [18, 21].

Fig. 3 displays the X-ray diffraction (XRD) pattern of the synthesized $LaFeO_3$ nanoparticles, confirming the formation of a well-crystallized orthorhombic perovskite phase. The diffraction peaks match well with the standard JCPDS card No. 37-1493 [22, 23], which corresponds to $LaFeO_3$. Prominent diffraction peaks are observed at 2θ values of approximately 22.9° (101), 32.2° (121), 39.6° (220), 46.1° (202), 52.3° (240), 57.4° (242), and 67.4° (400) planes, respectively. The most intense peak at around 32.2° is indexed to the (121) plane, which is characteristic of orthorhombic $LaFeO_3$ [23]. The sharp and well-defined peaks indicate that

the nanoparticles possess high crystallinity, while the absence of any extra peaks confirms the phase purity of the sample.

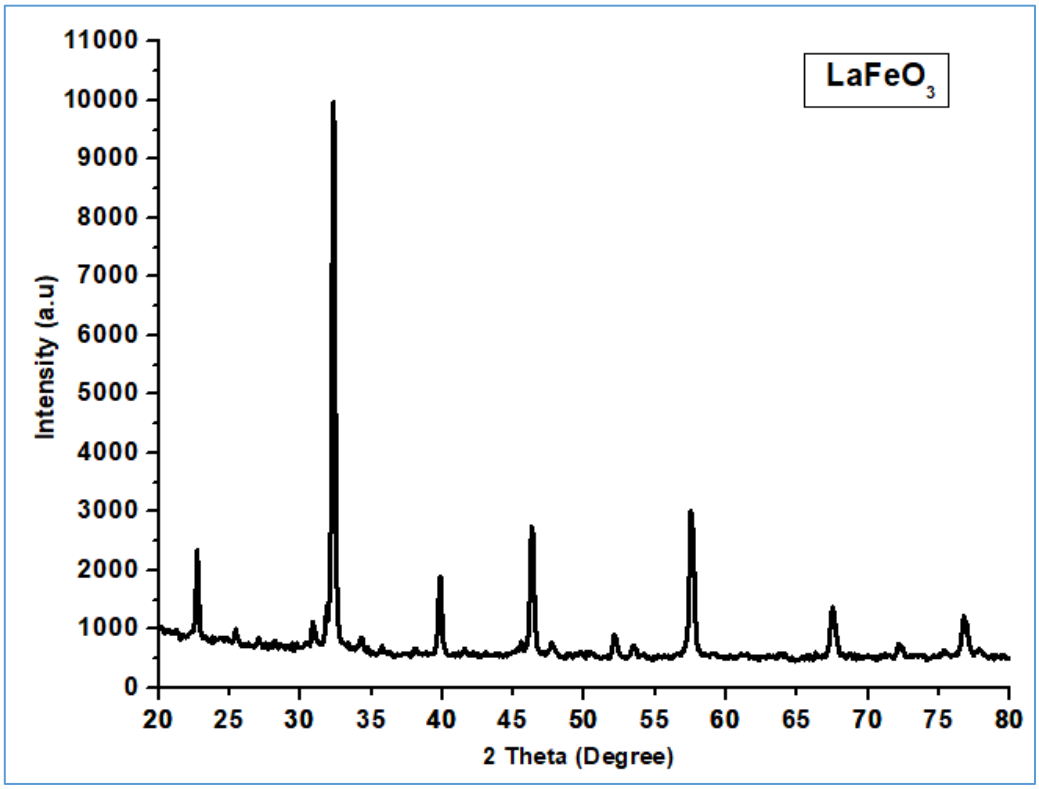

Fig. 3. XRD pattern of $LaFeO_3$ nanoparticles

The broadening of the diffraction peaks also suggests the nanocrystalline nature of the material, which is consistent with the crystallite size estimated using the Scherrer equation (Eq. 2) and found to be 46.89 nm, in good agreement with FESEM observations.

$$D = K\lambda / \beta \cos\Theta \qquad \text{(Eq. 2)}$$

Where,

D represents crystallite size, K represents Scherer constant (0.9), β represents full width at half maximum (FWHM), and λ denotes wavelength of X-ray source.

The indexing of these peaks to specific Miller indices (hkl planes) further validates the orthorhombic perovskite structure belonging to the Pnma space group. The XRD results strongly support the successful synthesis of phase-pure $LaFeO_3$ nanoparticles with orthorhombic symmetry and nanoscale crystallinity [23, 24].

Fig. 4 illustrates the temperature-dependent electrical resistance properties of $LaFeO_3$ nanoparticles. The resistance versus temperature plot (Fig. 4a) clearly shows that the resistance of the $LaFeO_3$ material decreases steadily with increasing temperature, indicating a negative temperature coefficient of resistance (NTCR), which is characteristic of semiconducting behavior. At lower temperatures (300–400 K), the resistance is relatively high (in the order of 10^9 Ω), suggesting limited charge carrier mobility due to carrier trapping and restricted hopping conduction. As the temperature increases above 400 K, the thermal energy supplied to the system becomes sufficient to excite charge carriers, enhancing their mobility and resulting in a sharp reduction in resistance. This confirms the semiconducting nature of $LaFeO_3$, where conduction is thermally activated [20, 21].

The corresponding Arrhenius-type plot, log Rc versus 1/T (Fig. 4b), provides deeper insight into the conduction mechanism. The graph shows a nearly linear relationship in the high-temperature region and determined by the Arrhenius equation (Eq.3). The resistivity was determined by Eq. 4 [21].

$$\Delta E = \frac{log\ R}{log\ Ro} \times KT \qquad \text{(Eq. 3)}$$

Where,

ΔE denotes activation energy, R represent resistance at raised temperature, R_0 is the resistance at room temperature.

$$\text{Resistivity} = \left(\frac{R \times b \times t}{l}\right)\Omega - m \qquad \text{(Eq. 4)}$$

Where,
R is resistance at normal temperature, b is breadth of film, t is thickness of the film, *l* is length of the film.

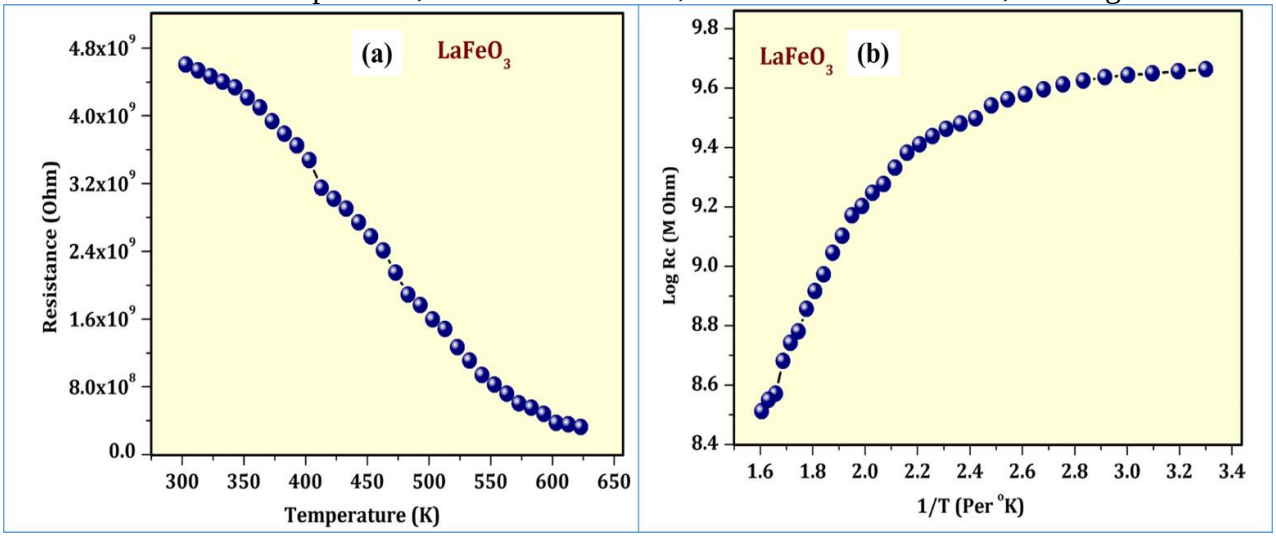

Fig. 4. Resistance versus temperature & (b) log Rc versus 1/T plot of $LaFeO_3$ nanoparticles

The linearity of the log Rc vs. 1/T plot suggests that the conduction process in $LaFeO_3$ is dominated by thermally activated hopping of charge carriers, particularly the movement of small polarons associated with oxygen vacancies and Fe^{3+}/Fe^{2+} redox couples. The electrical measurements confirm that $LaFeO_3$ behaves as a p-type semiconductor, where the increase in temperature significantly enhances conductivity by promoting hole transport and facilitating charge carrier hopping between Fe sites. Such thermal activation of conduction plays a crucial role in gas sensing applications, as the interaction between adsorbed oxygen species and target gases directly affects the charge carrier concentration and, consequently, the resistance of the sensing layer [20-22]. The thickness of film was estimated using mass difference method and thickness was found in micrometer. The electrical parameters of $LaFeO_3$ nanoparticle thick films are tabulated in Table 1.

Table 1. Electrical parameters of $LaFeO_3$ nanoparticle

Thick film	Thickness (μm)	Resistivity (Ω.m)	TCR (/°C)	Activation Energy (eV)	
				HTR	LTR
$LaFeO_3$	14	32237.6	-0.00378	0.1726	0.01409

The gas sensing properties of films were determined by using static gas sensing system [24]. In the presence of ethanol, SO_2, NH_3, LPG and CO gases at different operating temperature the sensitivity of films were measured. Fig. 5 summarizes the gas-sensing performance of the $LaFeO_3$ nanoparticle thick films.

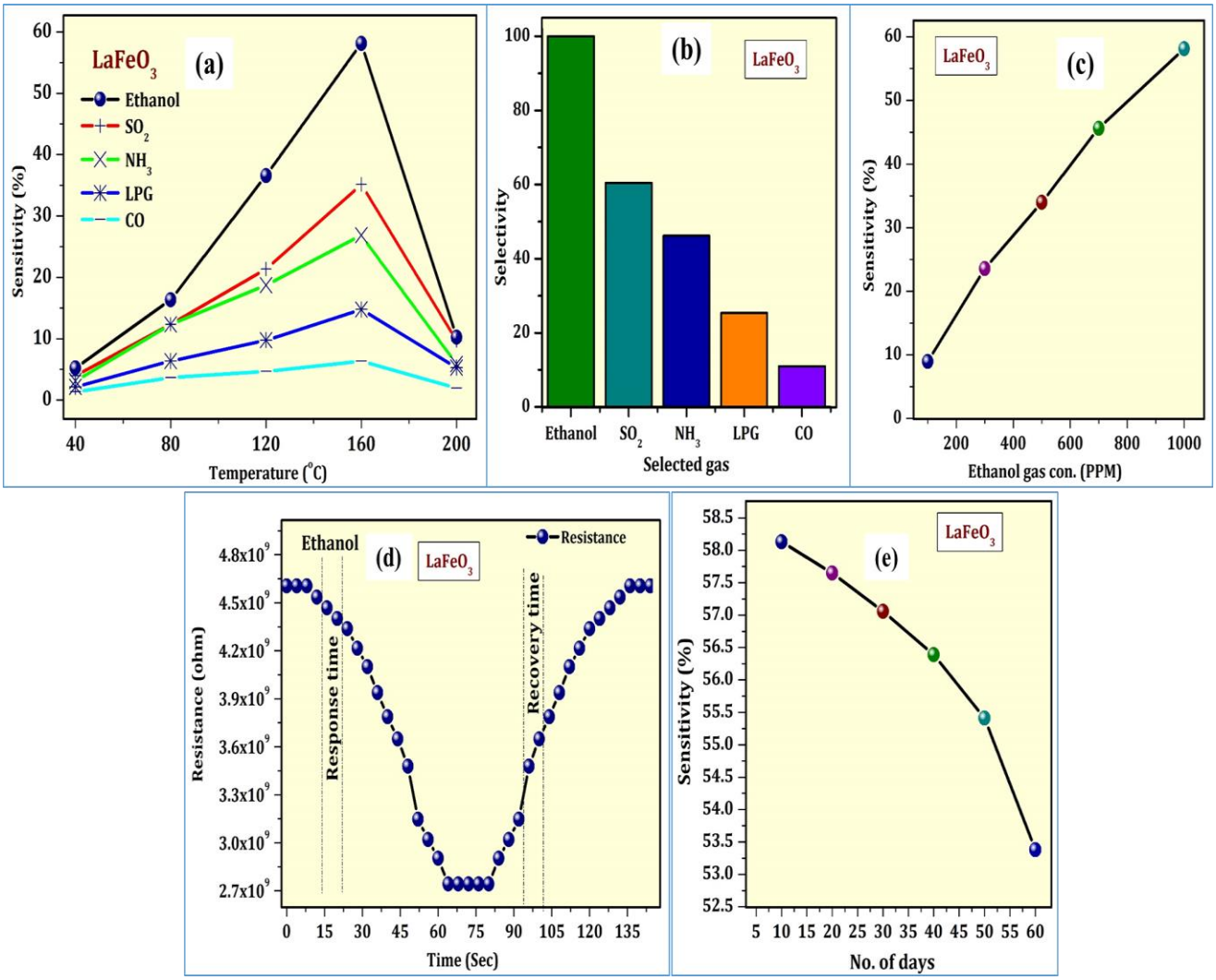

Fig. 5. (a) Sensitivity versus operating temperature, (b) selectivity histogram, (c) ppm variation, (d) response and recovery time & (d) reproducibility of $LaFeO_3$ nanoparticles

The temperature-dependent sensitivity plot (Fig. 5a) shows a clear optimum at 160 °C, ethanol sensitivity increases from 5.23% at 40 °C to 16.35% at 80 °C and 36.59% at 120 °C, reaches a maximum of 58.13% at 160 °C, then falls sharply to 10.25% at 200 °C. This behavior is typical of chemiresistive oxides at low temperatures adsorption and surface reaction rates are low sensitivity, at intermediate temperatures reaction kinetics and oxygen-ion activity are maximized sensitivity, and at excessively high temperatures desorption and reduced surface coverage dominate, lowering the response [25, 26]. The selectivity histogram (Fig. 5b), quantified relative to the ethanol response at 160 °C, confirms that the film is highly selective for ethanol gas, SO_2, NH_3, LPG and CO produce much lower responses at 160 °C (35.14%, 26.85%, 14.75% and 6.36% absolute sensitivities, respectively), which correspond to relative selectivities of ≈60%, ≈46%, ≈25% and ≈11% when normalized to ethanol (58.13% = 100%). The concentration dependence (Fig. 5c) is monotonic and nearly linear in the tested range: sensitivity rises from 8.95% (100 ppm) to 23.56% (300 ppm), 33.98% (500 ppm), 45.62% (700 ppm) and 58.13% (1000 ppm), indicating good dynamic range and predictable response with increasing ethanol concentration. The dynamic response trace (Fig. 5d) demonstrates fast and reversible chemiresistive behavior: upon exposure to 1000 ppm ethanol the resistance drops rapidly to a minimum (response time ≈ 23 s), then recovers toward baseline after gas removal with a recovery time of ≈103 s; the sharp resistance change and full recovery confirm fast surface reaction and desorption kinetics suitable for near-real-time monitoring [25-27]. The reproducibility/long-term stability data (Fig. 5e) show only a modest decline in sensitivity over two months: the ethanol sensitivity slightly decreases from 58.13% at day 10 to 57.65% (day 20), 57.06% (day 30), 56.39% (day 40), 55.41% (day 50) and 53.38% (day 60), i.e. an overall loss of ≈8.2% relative to the initial peak a small and acceptable deterioration that indicates reasonable device stability for practical sensing with periodic calibration. The films exhibit an optimal

operating temperature (160 °C), strong and selective ethanol response, good linear concentration dependence, rapid response and acceptable recovery, and stable performance over extended testing, all of which support their suitability for ethanol gas-sensing applications [27, 28].

The gas sensing mechanism of $LaFeO_3$ nanoparticles to ethanol gas is reveal in Fig. 6.

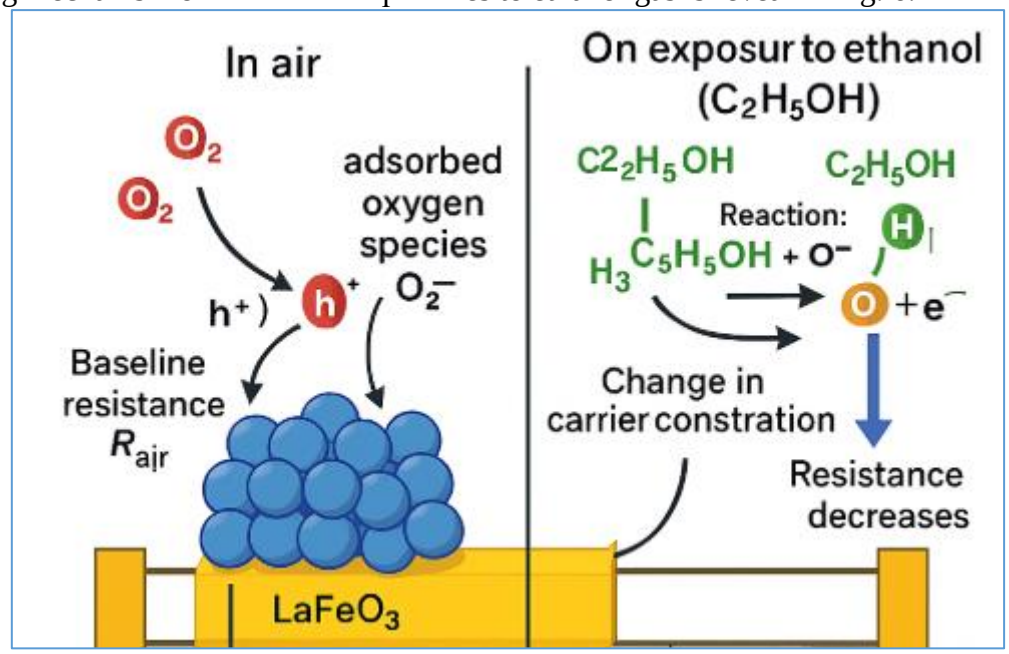

Fig. 6. Gas sensing mechanism of $LaFeO_3$ nanoparticles to ethanol gas

The sensing of ethanol by $LaFeO_3$ nanoparticles is driven by surface adsorption–reaction events. In air oxygen adsorbs and forms ionized species (predominantly O^- at the operating temperature ≈160 °C) that withdraw electrons and establish a baseline surface charge and resistance. Upon exposure to ethanol, the adsorbed oxygen oxidizes the ethanol, consuming the oxygen species and releasing electrons back into the material; this alters the near-surface carrier concentration and band-bending and produces a measurable change in resistance [25, 27]. The observed resistance decrease indicates that electron-injection or electron-dominated conduction channels prevail under these conditions, a behavior enhanced by the nanoscale grain size, porous morphology and Fe-centered catalytic sites that provide abundant active sites and rapid gas diffusion [28, 29].

CONCLUSIONS:

This work demonstrates a reliable sol–gel synthesis of phase-pure $LaFeO_3$ nanoparticles and their successful integration into screen-printed thick films for chemiresistive gas sensing. The orthorhombic perovskite $LaFeO_3$ as confirmed by XRD, with nanoscale crystallinity consistent with FESEM observations individual grains ≈40–72 nm) and a measured specific surface area of 2.06 $m^2 \cdot g^{-1}$. EDX mapping verified uniform elemental distribution (La, Fe, O). Electrical characterization revealed semiconducting NTCR behavior ($\rho \approx 3.22 \times 10^4\ \Omega \cdot m$, TCR ≈ −0.00378 $°C^{-1}$) and an estimated, low activation energy from the Arrhenius plot, these properties enable large relative resistance modulation upon gas interaction. Gas sensing tests established a clear optimum operating temperature of 160 °C with excellent sensitivity (58.13% at 1000 ppm ethanol), good selectivity toward ethanol over SO_2, NH_3, LPG and CO, fast dynamic response (≈23 s) and reasonable recovery (≈103 s), and acceptable reproducibility with only modest sensitivity decline over 60 days. The obtained results show that screen-printed $LaFeO_3$ thick films are promising, low-cost candidates for ethanol detection in environmental and industrial monitoring.

Acknowledgement

The authors gratefully acknowledge the Research Centre in Electronic Science, Mahatma Gandhi Vidyamandir's Loknete Vyankatrao Hiray Arts, Science and Commerce College, Panchavati, Nashik, affiliated to Savitribai Phule Pune University, Pune, Maharashtra – 422003, India, for providing the necessary facilities, instrumental support, guidance, and encouragement to carry out this research work. The authors

also acknowledge Savitribai Phule Pune University (SPPU), Pune, for access to characterization facilities and technical assistance.

REFERENCES:

1. Saxena, V. (2025). Water quality, air pollution, and climate change: investigating the environmental impacts of industrialization and urbanization. *Water, Air, & Soil Pollution*, *236*(2), 73.
2. Manisalidis, I., Stavropoulou, E., Stavropoulos, A., & Bezirtzoglou, E. (2020). Environmental and health impacts of air pollution: a review. *Frontiers in public health*, *8*, 14.
3. Sharma, S. B., Jain, S., Khirwadkar, P., & Kulkarni, S. (2013). The effects of air pollution on the environment and human health. *Indian Journal of Research in Pharmacy and Biotechnology*, *1*(3), 391.
4. Dhall, S., Mehta, B. R., Tyagi, A. K., & Sood, K. (2021). A review on environmental gas sensors: Materials and technologies. *Sensors International*, *2*, 100116.
5. Barik, P., & Pradhan, M. (2022). Selectivity in trace gas sensing: recent developments, challenges, and future perspectives. *Analyst*, *147*(6), 1024-1054.
6. Wang, H., Ma, J., Zhang, J., Feng, Y., Vijjapu, M. T., Yuvaraja, & Huang, J. (2021). Gas sensing materials roadmap. *Journal of Physics: Condensed Matter*, *33*(30), 303001.
7. Humayun, M., Li, Z., Israr, M., Khan, A., Luo, W., Wang, C., & Shao, Z. (2025). Perovskite type ABO3 oxides in photocatalysis, electrocatalysis, and solid oxide fuel cells: State of the art and future prospects. *Chemical Reviews*, *125*(6), 3165-3241.
8. Hjiri, M., Jbeli, A., Althumairi, N. A., Mustapha, N., & Aldukhayel, A. M. (2025). Ceramic perovskites via sol–gel processing: progress, challenges, and applications. *Journal of Sol-Gel Science and Technology*, 1-25.
9. Yadav, A. K., Singh, P., & Pandey, R. (2025). Advances in Lanthanum Ferrite-Based Sensors: A Comprehensive Review. *Analysis & Sensing*, *5*(4), e202400086.
10. Yadav, A. K., Kumar, U., & Yadav, B. C. (2025). Sol–gel-processed CNT-doped LaFeO3 and its application as LPG sensor. *Journal of Materials Science: Materials in Electronics*, *36*(1), 54.
11. Li, Q., Yang, B., Chen, X., Han, Y., Chen, Q., He, S., ... & Tang, J. (2024). Lanthanum ferrite modified filling materials and its enhancement for phosphorus and COD removal: Performance and mechanism. *Journal of Water Process Engineering*, *66*, 106015.
12. Wang, J., Liu, Q., Xue, D., & Li, F. (2002). Synthesis and characterization of LaFeO3 nano particles. *Journal of materials science letters*, *21*(13), 1059-1062.
13. Li, S., & Wang, X. (2015). Synthesis of different morphologies lanthanum ferrite (LaFeO3) fibers via electrospinning. *Optik*, *126*(4), 408-410.
14. Dumitru, R., Negrea, S., Ianculescu, A., Păcurariu, C., Vasile, B., Surdu, A., & Manea, F. (2020). Lanthanum ferrite ceramic powders: synthesis, characterization and electrochemical detection application. *Materials*, *13*(9), 2061.
15. Xu, Y. J., Song, S. Y., Li, C. X., Hong, B., Shi, D. S., Xu, J. C., ... & Wang, X. Q. (2021). Magnetic behavior, photocatalytic activity and gas-sensing performance of porous lanthanum ferrites powders. *Materials Chemistry and Physics*, *267*, 124628.
16. Meng, F., Yu, Z., Zhang, R., Gao, H., & Yuan, Z. (2024). Study of the Gas Sensing Performance of Ni-Doped Perovskite-Structured LaFeO3 Nanospheres. *Chemosensors*, *12*(4), 65.
17. Rammohan, K., VijayaLakshmi, G., Ramesh, G., & Tiwari, S. (2025). SYNTHESIS AND CHARACTERIZATION OF $AgLaFeO_3$ PEROVSKITE VIA A SIMPLE SOL-GEL METHOD AND INVESTIGATION OF ITS MAGNETIC PROPERTIES. *Rasayan Journal of Chemistry*, *18*(2).
18. Koli, P. B., Kapadnis, K. H., Deshpande, U. G., Tupe, U. J., Shinde, S. G., & Ingale, R. S. (2021). Fabrication of thin film sensors by spin coating using sol-gel LaCrO3 Perovskite material modified with transition metals for sensing environmental pollutants, greenhouse gases and relative humidity. *Environmental Challenges*, *3*, 100043.
19. Suryawanshi, P. S., Patil, A. V., Padhye, G. G., & Tupe, U. J. (2024). Investigation the Influence of Calcination Temperature on Structural, Electrical and Gas Sensing Properties MnO2 Thick Films. *Advanced Materials Research*, *1180*, 67-81.

20. Wagh, S. L., Tupe, U. J., Patil, A. B., & Patil, A. V. (2022). Influence of Annealing Temperature on Structural and Electrical Properties of Screen Printed Lanthanum Oxide Thick Films. *Iranian Journal of Materials Science & Engineering*, *19*(4).
21. Lad, U. D., Kokode, N. S., & Tupe, U. J. (2022). Study of pn Heterojunction Thin Films for Reducing Gas Sensing Application Fabricated by Thermal Evaporation Technique. *Advanced Materials Research*, *1172*, 67-82.
22. Li, F. T., Liu, Y., Liu, R. H., Sun, Z. M., Zhao, D. S., & Kou, C. G. (2010). Preparation of Ca-doped LaFeO3 nanopowders in a reverse microemulsion and their visible light photocatalytic activity. *Materials Letters*, *64*(2), 223-225.
23. Gabal, M. A., Al-Solami, F., Al Angari, Y. M., Ali, A. A., Al-Juaid, A. A., Huang, K. W., & Alsabban, M. (2019). Auto-combustion synthesis and characterization of perovskite-type LaFeO3 nanocrystals prepared via different routes. *Ceramics International*, *45*(13), 16530-16539.
24. Koli, P. B., Kapadnis, K. H., Deshpande, U. G., More, B. P., & Tupe, U. J. (2020). Sol-gel fabricated transition metal Cr3+, Co2+ doped lanthanum ferric oxide (LFO-LaFeO3) thin flm sensors for the detection of toxic, fammable gases: a comparative study. *Mater Sci Res India*, *17*, 70-83.
25. Li, F., Wang, S., Wu, Z., Xiong, X., Li, J., Zhou, J., & Gao, X. (2021). Excellent ethanol sensor based on LaFeO3 modified with gold nanoparticles. *Journal of Materials Science: Materials in Electronics*, *32*(23), 27587-27595.
26. Xiang, J., Chen, X., Zhang, X., Gong, L., Zhang, Y., & Zhang, K. (2018). Preparation and characterization of Ba-doped LaFeO3 nanofibers by electrospinning and their ethanol sensing properties. *Materials Chemistry and Physics*, *213*, 122-129.
27. Qin, W., Zhang, R. Meng, F. (2022). Preparation of P-$LaFeO_3$/n-Fe_2O_3 heterojunction composites by one-step hydrothermal method and gas sensing properties for acetone. IEEE Transactions on Instrumentation and Measurement, 71, 1-9.
28. Meng, F., Yu, Z., Zhang, R., Gao, H., & Yuan, Z. (2024). Study of the Gas Sensing erformance of Ni-Doped Perovskite-Structured LaFeO3 Nanospheres. Chemosensors, 12(4), 65.
29. Cao, E., Chu, Z., Wang, H., Hao, W., Sun, L., & Zhang, Y. (2018). Effect of film thickness on the electrical and ethanol sensing characteristics of LaFeO3 nanoparticle-based thick film sensors. *Ceramics International*, *44*(6), 7180-7185.